Inorganic Chemistry

Article

pubs.acs.org/IC

Ruthenium(II) Thiol and H_2S Complexes: Synthesis, Characterization, and Thermodynamic Properties

Erin S. F. Ma, Steven J. Rettig,† Brian O. Patrick, and Brian R. James*

Department of Chemistry, University of British Columbia, Vancouver, British Columbia V6T 1Z1, Canada

Supporting Information

ABSTRACT: The known, green, five-coordinate species *trans*-$RuCl_2(P{-}N)(PPh_3)$ react with R′SH thiols to give yellow *cis*-$RuCl_2(P{-}N)(PPh_3)(R'SH)$ products (P−N = *o*-diphenylphosphino-*N*,*N*′-dimethylaniline; R′ = alkyl). The MeSH and EtSH compounds are structurally characterized, with the former being the first reported for a transition metal−MeSH complex, while the thiol complexes with R′ = ^{n}Pr, ^{i}Pr, ^{n}Pn (pentyl), ^{n}Hx (hexyl), and Bn (benzyl) are synthesized in situ. Other *trans*-$RuX_2(P{-}N)(PR_3)$ complexes (X = Br, I; R = Ph, *p*-tolyl) are synthesized, and their H_2S adducts, of a type reported earlier by our group, are also prepared. Thermodynamic data are presented for the reversible formation of the MeSH and EtSH complexes and the H_2S analogues. The $Ru^{II}Cl_2(P{-}N)(PPh_3)$ complex in solution decomposes under O_2 to form $[Ru^{III}Cl(P{-}N)]_2(\mu\text{-}O)(\mu\text{-}Cl)_2$.

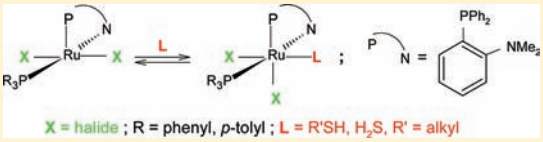

INTRODUCTION

Our group has recently reported on thiol complexes of the formulation *trans*- $Ru^{II}(porp)(RSH)_2$, where porp represents the dianionic ligand of a porphyrin and R is an alkyl or phenyl group;[1] this paper also discusses the potential of these complexes as models for Fe−S bonds in heme proteins because systems that contain proximal S-donor ligands at a heme center are involved in many biological catalytic and/or structural processes.[2] The studies required an extensive literature search for metal−thiol complexes, and it became clear that examples of coordinated thiols (and H_2S), in general, are relatively rare, especially structurally characterized species. This is because the attempted coordination of thiols (and H_2S) commonly results in the formation of the respective thiolato/hydrosulfide ligand via deprotonation, or hydridothiolato species via oxidative addition, with the thiol or H_2S adduct usually considered as an intermediate.[3]

The recent study[1] brought to mind earlier work from our group on thiol binding to Ru^{II} that was completed in the late 1990s; however, this was never published and so is presented here. The findings evolve from the reactivity of the five-coordinate species *trans*-$RuCl_2(P{-}N)(PR_3)$ toward small molecules, where P−N = *o*-diphenylphosphino-*N*,*N*′-dimethylaniline (see eq 1) and R = phenyl or *p*-tolyl.[4,5] The structurally

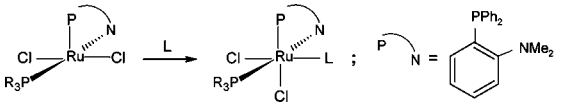

(1)

characterized *p*-tolyl complex has approximately square-pyramidal geometry with *trans*-chlorides, the monodentate phosphine, and $-NMe_2$ in the equatorial positions and the chelate P atom in the apical position.[4] We have published details on the coordination of H_2, N_2, H_2S, and N_2O (defined here as L) at the vacant site to generate *cis*-$RuCl_2(P{-}N)(PR_3)L$ complexes (eq 1).[4,5] These papers[4,5] mention in a sentence the coordination of thiols, alcohols, H_2O, CO, and SO_2, but the chemistry of these systems has been described only in Ph.D. dissertations and at a conference.[6] This current paper focuses mainly on the thiol products, including crystallographic data for the L = MeSH and EtSH complexes, and compares their properties with those of the corresponding H_2S adduct.[5] The structure with MeSH is surprisingly the first reported for any transition-metal complex containing this thiol.

There are about one dozen reported structures of ruthenium thiol complexes, in which the thiol contains no other functional binding sites. Some of these structures are included in several reports[7] on $CpRu^{II}$-RSH complexes, exemplified by $[CpRu(PPh_3)_2(RSH)]^+$, where R is a range of alkyl groups (including Me and Ph); structures of this type (sometimes containing other phosphines or phosphites) are with R = ^{n}Pr,[7a] ^{t}Bu,[7b] ^{s}Bu,[7f] ^{i}Bu,[7f] $PhCH_2CH_2$,[7e] Ph,[7g] and PhCH(SH)Me.[7h] Structures of $Ru(H)_2(CO)(IMes)_2(^n PrSH)$[8] and $Ru(porp)(CPh_2)(EtSH)$[9] containing carbene ligands have also been reported [IMes = 1,3-(2,4,6-trimethylphenyl)imidazol-2-ylidene and porp = dianion of *meso*-tetrakis(pentafluorophenyl)porphyrin], although the former was later shown to be a hydridothiolato complex.[8b] Other ruthenium thiol complexes, not structurally characterized, include the 2,7-dimethyloctadienediyl species $[(\eta^3{:}\eta^3\text{-}C_{10}H_{16})Ru^{IV}Cl_2(RSH)]$ (R = Me, Et, ^{i}Pr, ^{t}Bu, Ph),[10] and the 1,2-bis(diphenylphosphino)ethane species *trans*-$[Ru(H)(PhSH)(dppe)_2]^+$, which was made by protonation of the neutral thiolate species using HBF_4;[11] similarly made were the related pyridine-2- and quinoline-8-thiol species.[12]

Received: February 22, 2012
Published: April 11, 2012

   dx.doi.org/10.1021/ic3004118 | *Inorg. Chem.* 2012, 51, 5427−5434

EXPERIMENTAL SECTION

General Procedures. Unless stated otherwise, all manipulations were performed under an O_2-free, Ar or N_2 atmosphere at ambient temperatures using standard Schlenk techniques. Commercially available compounds, including the thiols, $SPPh_3$, and $OPPh_3$, were supplied by Aldrich; MeSH was obtained as a liquid and was stored at 0 °C. Anhydrous H_2S was obtained from Matheson Gas Co. and O_2 (USP grade) from Union Carbide Canada Ltd. The thiols and H_2S were used as received. Spectral- or analytical-grade solvents were refluxed, distilled over appropriate drying agents,[13] and then purged free of O_2 prior to use. Deuterated solvents, obtained from Cambridge Isotope Laboratories, were stored over activated molecular sieves (Fisher, 4 Å, 4–8 mesh); for the preparation of O_2-sensitive complexes, the deuterated solvents were deoxygenated (via a freeze–pump–thaw method) and stored under Ar. Reactions with the odoriferous and toxic materials, especially H_2S and MeSH (bp 6 °C), were carried out in a well-ventilated fumehood.

NMR spectra were recorded, unless stated otherwise, at room temperature (rt ~ 25 °C) on Varian XL300 (300.0 MHz for ^1H and 121.4 MHz for ^{31}P) or Bruker AMX500 (500.0 MHz for ^1H and 202.5 MHz for ^{31}P) instruments. Residual deuterated solvent proton (relative to external $SiMe_4$) or external $P(OMe)_3$ (δ 141.0 relative to 85% H_3PO_4) was used as a reference (s = singlet, d = doublet, t = triplet, q = quartet, and m = multiplet); J values are reported in hertz (Hz); samples were prepared in 5 mm NMR tubes equipped with poly(tetrafluoroethylene) and J. Young valves (Aldrich). Calibrated ^1H NMR probes were used to determine the temperatures used for van't Hoff analyses. ATLI Mattson Genesis FTIR and Bomem Michelson far-IR spectrophotometers were used to record spectra in the ranges 500–4000 cm^{-1} (KBr) and 200–3000 cm^{-1} (CsI). UV–vis spectra were recorded on a Hewlett-Packard 8452A diode-array spectrophotometer, equipped with a thermostatted compartment using an anaerobic 1 cm quartz cell, joined to a side-arm flask for the mixing of solutions. Differential scanning calorimetry (DSC) data were collected on a TA 910S instrument, with 2–5 mg samples being heated under N_2 (flow rate = 40 cm^3 min^{-1}) at a rate of 5 °C min^{-1} up to 500 °C. Microanalyses were performed in this department on a Carlo Erba 1106 instrument.

The complexes $RuCl_2(PR_3)_3$ (R = Ph,[14] *p*-tolyl[15]), $RuX_2(P–N)(PPh_3)$ [X = Cl (**1a**),[4a] Br (**1b**)];[5b] $RuCl_2(P–N)(P(p\text{-tolyl})_3)$ (**1a′**);[4a] *cis*-$RuX_2(P–N)(PPh_3)(SH_2)$ [X = Cl (**2a**), Br (**2b**)];[5b] and *cis*-$RuCl_2(P–N)(P(p\text{-tolyl})_3)(SH_2)$ (**2a′**)[4a] were prepared by literature methods. Complexes **2a**, **2b**, and **2a′** were all isolated with an acetone solvate molecule. [**a**–**c** labeling indicates PPh_3 complexes with chloro, bromo, and iodo ligands, respectively; the corresponding $P(p\text{-tolyl})_3$ complexes are labeled **a′**–**c′**; the five-coordinate precursors are all labeled **1**, and the H_2S adducts are correspondingly labeled **2**.]

$RuX_2(P–N)(PR_3)$ Complexes. The new complexes $RuI_2(P–N)(PPh_3)$ (**1c**) and $RuX_2(P–N)(P(p\text{-tolyl})_3)$ [X = Br (**1b′**), I (**1c′**)] were prepared by a method similar to that used for the PPh_3 analogues **1a** and **1b**.[4a,5b] A solution of P–N (0.44 mmol) in acetone (10 mL) was added to a suspension of $RuCl_2(PR_3)_3$, where R = Ph or *p*-tolyl (0.44 mmol), in acetone (10 mL), and the mixture was stirred at 50 °C for 30 min. Excess NaX (25 equiv) was then added to the resulting dark-green solution. The mixture, containing a suspension of NaX and NaCl, was stirred at rt for 24 h. The salts were filtered off through Celite, and the solvent was removed in vacuo; CH_2Cl_2 (10 mL) was then added to dissolve the dark-green (Br species) or dark-red residue (I species), and the solution was filtered through Celite. The filtrate volume was reduced to ~5 mL before hexanes was added to precipitate the product that was filtered off and washed with hexanes (2 × 10 mL); drying under vacuum gave the products in 51–86% yield. Previously unreported elemental analysis and NMR data for **1b** are given below.

*$RuBr_2(P–N)(PPh_3)$ (**1b**).* Yield: 185 mg, 51%. Anal. Calcd for $C_{38}H_{35}NBr_2P_2Ru$: C, 55.09; H, 4.26; N, 1.69. Found: C, 54.57; H, 4.23; N, 1.64. $^{31}P\{^1H\}$ NMR (C_6D_6): δ 85.47 (d, P_N, $^2J_{PP}$ = 36.3 Hz), 50.08 (d, P, $^2J_{PP}$ = 36.3 Hz). ^1H NMR (C_6D_6): δ 7.8–6.7 (29H, m, Ph), 3.17 (6H, s, $N(CH_3)_2$). [P_N and P refer to the P–N and PPh_3 ligands respectively.]

*$RuI_2(P–N)(PPh_3)$ (**1c**).* Yield: 348 mg, 86%. Anal. Calcd for $C_{38}H_{35}NI_2P_2Ru$: C, 49.47; H, 3.82; N, 1.52. Found: C, 49.21; H, 3.78; N, 1.58. $^{31}P\{^1H\}$ NMR ($CDCl_3$): δ 89.18 (d, P_N, $^2J_{PP}$ = 35.56 Hz), 53.6 (d, P, $^2J_{PP}$ = 35.56 Hz). ^1H NMR ($CDCl_3$): δ 7.8–6.9 (29H, m, Ph), 3.48 (6H, s, $N(CH_3)_2$).

*$RuBr_2(P–N)(P(p\text{-tolyl})_3)$ (**1b′**).* Yield: 202 mg, 53%. Anal. Calcd for $C_{41}H_{41}NBr_2P_2Ru$: C, 56.56; H, 4.75; N, 1.61. Found: C, 57.09; H, 4.86; N, 1.75. $^{31}P\{^1H\}$ NMR ($CDCl_3$): δ 84.56 (d, P_N, $^2J_{PP}$ = 35.5 Hz), 47.48 (d, P, $^2J_{PP}$ = 35.5 Hz). ^1H NMR ($CDCl_3$): δ 8.0–6.6 (26H, m, Ph), 3.12 (6H, s, $N(CH_3)_2$), 2.30 (9H, s, *p*-CH_3).

*$RuI_2(P–N)(P(p\text{-tolyl})_3)$ (**1c′**).* Yield: 300 mg, 72%. Anal. Calcd for $C_{41}H_{41}NI_2P_2Ru$: C, 51.05; H, 4.28; N, 1.45. Found: C, 51.05; H, 4.25; N, 1.48. $^{31}P\{^1H\}$ NMR ($CDCl_3$): δ 89.27 (d, P_N, $^2J_{PP}$ = 35.8 Hz), 51.27 (d, P, $^2J_{PP}$ = 35.8 Hz). ^1H NMR ($CDCl_3$): δ 7.8–6.7 (26H, m, Ph), 3.46 (6H, s, $N(CH_3)_2$), 2.30 (9H, s, *p*-CH_3).

***cis*-$RuBr_2(P–N)(P(p\text{-tolyl})_3)(SH_2)$ (2b′).** This complex was prepared in a manner similar to that described for **2a**,[5b] by stirring **1b′** (100 mg, 0.11 mmol) in acetone (3 mL) under 1 atm of H_2S at rt. The precipitated yellow product was filtered off and subsequently dried under vacuum for 1 h. Yield: 86 mg, 78%. Anal. Calcd for $C_{41}H_{43}NBr_2SP_2Ru$·acetone: C, 54.89; H, 5.13; N, 1.45. Found: C, 55.11; H, 5.23; N, 1.49. $^{31}P\{^1H\}$ NMR ($CDCl_3$): δ 53.41 (d, P_N, $^2J_{PP}$ = 29.2 Hz), 44.58 (d, P, $^2J_{PP}$ = 29.2 Hz). ^1H NMR ($CDCl_3$): δ 8.0–6.6 (26H, m, Ph), 3.68 (3H, s, NCH_3), 2.99 (3H, s, NCH_3), 2.18 (9H, s, *p*-CH_3), 2.04 (6H, s, acetone), 0.95 (2H, br s, SH_2). IR: ν_{SH} 2495 s, 2449 s; ν_{CO} 1707 (acetone).

In Situ Syntheses of *cis*-$RuI_2(P–N)(PR_3)(SH_2)$ (R = Ph, *p*-tolyl). Exposure of a $CDCl_3$ solution of $RuI_2(P–N)(PR_3)$ to 1 atm H_2S at rt turned the color from red to brown; NMR spectra were measured within 10 min because the in situ species decomposed over ~1 h, with generation of broad-line spectra.

*R = Ph (**2c**).* $^{31}P\{^1H\}$ NMR: δ 56.0 (d, P_N, $^2J_{PP}$ = 25.8 Hz), 49.5 (d, P, $^2J_{PP}$ = 25.8 Hz). ^1H NMR: δ 8.2–6.5 (29H, m, Ph), 4.16 (3H, s, NCH_3), 2.20 (3H, s, NCH_3), ~0.95 (SH_2, overlapping with the δ 1.0 signal of free H_2S).

*R = p-tolyl (**2c′**).* $^{31}P\{^1H\}$ NMR: δ 56.2 (d, P_N, $^2J_{PP}$ = 25.8 Hz), 47.5 (d, P, $^2J_{PP}$ = 25.8 Hz). ^1H NMR: δ 8.2–6.5 (26H, m, Ph), 4.15 (3H, s, NCH_3), 2.91 (3H, s, NCH_3), 2.22 (9H, s, *p*-CH_3), ~0.90 (SH_2, overlapping with the δ 1.0 signal of free H_2S).

***cis*-$RuCl_2(P–N)(PPh_3)$(MeSH) (3).** A solution of MeSH (0.5 mL, 9.0 mmol) in acetone (2 mL) was cooled to 0 °C, purged with N_2 for 1 min, and then cannula-transferred to a stirring acetone solution (5 mL) containing $RuCl_2(PPh_3)_3$ (100 mg, 0.104 mmol) and P–N (32.0 mg, 0.104 mmol); the resulting yellow solution, after being stirred for 16 h, precipitated a solid, which was filtered off and dried in vacuo for 30 min. Yield: 72 mg, 80%. Anal. Calcd for $C_{39}H_{39}NCl_2SP_2Ru$·acetone: C, 59.64; H, 5.36; N, 1.66. Found: C, 59.46; H, 5.53; N, 1.65. $^{31}P\{^1H\}$ NMR (CD_2Cl_2): δ 50.37 (d, P_N, $^2J_{PP}$ = 30.2 Hz), 41.33 (d, P, $^2J_{PP}$ = 30.2 Hz). ^1H NMR (CD_2Cl_2): δ 7.9–6.4 (29H, m, Ph), 3.35 (3H, s, NCH_3), 3.10 (3H, s, NCH_3), 2.10 (6H, s, acetone), 0.70 (4H, m, overlap of $SH(CH_3)$ and $SH(CH_3)$). IR: ν_{SH} 2533 s, ν_{CO} 1707 s (acetone). Yellow-brown, prism crystals of **3**·acetone were obtained from a saturated acetone solution of the complex left standing for 24 h.

***cis*-$RuCl_2(P–N)(PPh_3)$(EtSH) (4).** The yellow complex was prepared in the manner described for **3** but using excess EtSH (1 mL, 19.2 mmol) at 20 °C. Yield: 65 mg, 78%. Anal. Calcd for $C_{40}H_{41}NCl_2SP_2Ru$·acetone: C, 58.62; H, 5.79; N, 1.52. Found: C, 59.08; H, 5.75; N, 1.46. $^{31}P\{^1H\}$ NMR (CD_2Cl_2): δ 52.43 (d, P_N, $^2J_{PP}$ = 30.2 Hz), 43.97 (d, P, $^2J_{PP}$ = 30.2 Hz). ^1H NMR (CD_2Cl_2): δ 8.0–6.4 (29H, m, Ph), 3.41 (3H, s, NCH_3), 3.24 (3H, s, NCH_3), 2.10 (6H, s, acetone), 2.00 (1H, m, $SH_a(CH_bH_cCH_3)$), 0.88 (1H, m, $SH(CH_bH_cCH_3)$), 0.63 (1H, ddd, $SH_a(CH_bH_c)$), 0.45 (3H, dd, $SH(CH_aH_bCH_3)$); free EtSH signals seen at δ 2.55 (2H, dq, $HSCH_2CH_3$), 1.46 (1H, t, $HSCH_2CH_3$), 1.31 (3H, t, $HSCH_2CH_3$). IR: ν_{SH} 2516 s, ν_{CO} 1707 s (acetone). Yellow, prism crystals of **4**·1.5C_6H_6 were obtained from a saturated C_6H_6 solution of the complex left in a sealed NMR tube for 24 h.

dx.doi.org/10.1021/ic3004118 | *Inorg. Chem.* 2012, 51, 5427–5434

In Situ Syntheses of *cis*-$RuCl_2(P-N)(PPh_3)(R'SH)$ [R′ = ^{n}Pr, ^{i}Pr, ^{n}Pn (pentyl), ^{n}Hx (hexyl), Bn (benzyl)]. These yellow species were prepared in situ by the addition of ∼100-fold excess thiol to a $CDCl_3$ or C_6D_6 solution of $RuCl_2(P-N)(PPh_3)$. $^{31}P\{^1H\}$ NMR data are summarized as follows. R = ^{n}Pr. NMR ($CDCl_3$): δ 51.22 (d, P_N, $^2J_{PP}$ = 30.1 Hz), 42.46 (d, P, $^2J_{PP}$ = 30.1 Hz). R = ^{i}Pr. NMR (C_6D_6): δ 49.58 (d, P_N, $^2J_{PP}$ = 30.2 Hz), 41.68 (d, P, $^2J_{PP}$ = 30.2 Hz). R = ^{n}Pn. NMR (C_6D_6): δ 51.30 (d, P_N, $^2J_{PP}$ = 29.6 Hz), 42.84 (d, P, $^2J_{PP}$ = 29.6 Hz). R = ^{n}Hx. NMR ($CDCl_3$): δ 51.15 (d, P_N, $^2J_{PP}$ = 30.2 Hz), 42.57 (d, P, $^2J_{PP}$ = 30.2 Hz). R = Bn. NMR ($CDCl_3$): δ 50.16 (d, P_N, $^2J_{PP}$ = 30.4 Hz), 42.03 (d, P, $^2J_{PP}$ = 30.4 Hz).

$[RuCl(P-N)]_2(\mu$-O)(μ-Cl)$_2$ (5). A suspension of $RuCl_2(P-N)(PPh_3)$ (200 mg, 0.270 mmol) in acetone (10 mL) was stirred for ∼1 h under 1 atm of O_2 to give a dark-green solution. Continued stirring for ∼16 h generated a dark-green solid, which was filtered off, washed with hexanes (2 × 10 mL), and dried in vacuo at 80 °C. Yield: 85 mg, 32%. Anal. Calcd for $C_{40}H_{40}N_2OCl_4P_2Ru_2$: C, 49.50; H, 4.15; N, 2.89. Found: C, 49.50; H, 4.16; N, 2.75. $^{31}P\{^1H\}$ NMR (C_6D_6): δ 38.74 (d, P_N, $^4J_{PP}$ = 10.4 Hz), 35.33 (d, P_N, $^4J_{PP}$ = 10.4 Hz). ^1H NMR (C_6D_6): δ 8.4−6.6 (28H, m, Ph), 3.31 (3H, s, NCH_3), 2.89 (3H, s, NCH_3), 2.11 (3H, s, NCH_3), 2.02 (3H, s, NCH_3). μ_{eff} = 0 μ_B (Gouy method). Dark-green, platelet crystals of **5**·acetone were obtained by slow evaporation in air of an acetone solution of $RuCl_2(P-N)(PPh_3)$ over 24 h; the X-ray structure was reported in an earlier communication from our group.[4b]

X-ray Crystallographic Analyses. Data for the structures of the solvated complexes **3** and **4** were collected on a Rigaku/ADSC CCD area detector with graphite-monochromated Mo Kα radiation (λ = 0.71069 Å) at 180 K and processed using the *d*TREK* area detector program;[16] the structures were solved by direct methods.[17] All refinements were performed using the *SHELXL-97* program[18] via the *WinGX* interface.[19] The non-H atoms were refined anisotropically; the H atoms of the S−H moieties were refined isotropically, and the rest of the H atoms were fixed in idealized, calculated positions.

Crystal data for $C_{42}H_{45}Cl_2NOP_2RuS$ (**3**·acetone): M = 845.81; yellow-brown prisms; crystal size 0.13 × 0.25 × 0.35 mm; monoclinic, space group $P2_1/n$ (No. 4); a = 14.207(1) Å, b = 16.275(2) Å, c = 16.712(3) Å; β = 92.667(1)°; V = 3860.1(9) Å^3; Z = 4; D_c = 1.455 g cm^{-3}; $F(000)$ = 1744; μ = 7.16 cm^{-1}; 36449 total reflections; 9923 unique (R_{int} = 0.061); 8391 observed [$I > 2\sigma(I)$], $R(F)$ = 0.055; $R_w(F^2$, all data) = 0.126; GOF = 1.18; residual density = −1.50 e/Å^3.

Crystal data for $C_{49}H_{50}Cl_2NP_2RuS$ (**4**·1.5C_6H_6): M = 918.92; yellow prisms; crystal size 0.30 × 0.30 × 0.20 mm; monoclinic, space group $P2_1/n$ (No. 4); a = 16.6933(8) Å, b = 12.426(1) Å, c = 21.8288(6) Å; β = 106.331(1)°; V = 4345.3(5) Å^3; Z = 4; D_c = 1.405 g cm^{-3}; $F(000)$ = 1900; μ = 6.41 cm^{-1}; 39270 total reflections; 11499 unique (R_{int} = 0.031); 8808 observed [$I > 2\sigma(I)$], $R(F)$ = 0.033; $R_w(F^2$, all data) = 0.089; GOF = 1.06; residual density = −0.66 e/Å^3.

RESULTS AND DISCUSSION

$RuX_2(P-N)(PR_3)$ Complexes and Their H_2S Adducts. Green, five-coordinate complexes of the type $RuX_2(P-N)(PR_3)$, where X = halogen and R = Ph or *p*-tolyl, and some of their yellow H_2S adducts (eq 1), have been reported previously.[4,5] The new analogues, $RuI_2(P-N)(PPh_3)$ (**1c**), $RuX_2(P-N)(P(p\text{-tolyl})_3)$ [X = Br (**1b′**), I (**1c′**)], and *cis*-$RuX_2(P-N)(PR_3)(SH_2)$ [R = Ph, X = I (**2c**); R = *p*-tolyl; X = Br (**2b′**), I (**2c′**)] were prepared by similar procedures. The isolated **1c**, **1b′**, and **1c′** were made by reacting $RuCl_2(PR_3)_3$ with the P−N ligand in the presence of NaX (X = Br, I) in acetone. Reaction of the appropriate precursor with H_2S in solution gave the H_2S adduct; **2b′** was isolated as an acetone-solvated complex, while **2c** and **2c′** were formed in situ in $CDCl_3$. The $^{31}P\{^1H\}$ and ^1H NMR spectra of the five-coordinate species are essentially the same as those reported earlier for the chloro analogues:[4a,5] an AX pattern with $^2J \sim 35$ Hz for the *cis*-P atoms,[4a] and a singlet for NMe_2, respectively. The NMR data for the H_2S adducts (an AX $^{31}P\{^1H\}$ pattern with $^2J \sim 26-30$ Hz and two singlets in the ^1H NMR spectrum for inequivalent Me groups) are again close to those of the previously reported analogues.[5] An extension of the Karplus relationship to vicinal coupling within the P−Ru−S−H system was demonstrated previously for this type of complex, specifically within the *cis*-$RuX_2(P-N)(PPh_3)(SH_2)$ complexes, where X = Cl (**2a**) and Br (**2b**).[5b] Crystallographically characterized metal−H_2S complexes remain limited to just five ruthenium(II) species.[5,20]

***cis*-$RuCl_2(P-N)(PPh_3)(R'SH)$.** These thiol complexes [R′ = Me (**3**), Et (**4**)], like the H_2S adducts, slowly precipitated spontaneously out of solutions containing R′SH and excess thiol. Both **3** and **4** were fully characterized and are isostructural with the corresponding H_2S adduct.[5b] The ORTEP plots (Figures 1 and 2) show pseudooctahedral geometries with *cis*-Cl atoms and *cis*-P atoms, with the coordinated thiol trans to a Cl atom and cis to both P atoms and the NMe_2; selected bond lengths and angles are shown Tables 1 and 2, respectively. A search of the Cambridge Structural Database indicates that **3** is the first structure of a transition metal−MeSH complex. The S−H bond length of 1.06(4) Å is the shortest yet reported for any transition metal−thiol complex; this bond length for **4** is 1.28(2) Å, intermediate between those of 1.20(3) and 1.30(3) Å seen for the H_2S analogue **2a**;[5b] reported S−H bond lengths of other ruthenium(II) thiol complexes are in the 1.18−1.38 Å range.[7a,e−g] The Ru−S bond length in both **3** and **4** is 2.34 Å, and for **2a**, the length is 2.35 Å.[5b] These values are at the low end of the 2.34−2.42 Å range reported for all other structurally characterized ruthenium(II) thiols (see the Introduction section), except one.[7a,b,e−h,9] The exception is Ru(porp)-(CPh_2)(EtSH), where the value is 2.75 Å,[9] and this could result from steric interactions with the pentafluorophenyl substituents of the porphyrin ligand and/or the trans influence of the carbene ligand. The Ru−S−H angles of 102(2)° and 109.1(11)° for **3** and **4**, respectively, are close to those observed for the H_2S adduct, 103(1)° and 111(1)°. Both the alkyl and H of the R′SH ligand in **3** and **4** are situated below the S−P−Cl−

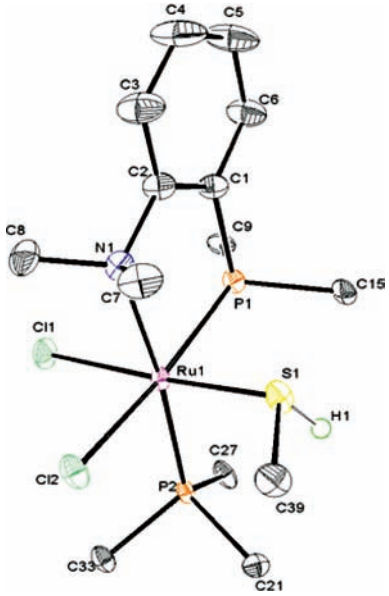

Figure 1. ORTEP plot for **3** with thermal ellipsoids shown at the 33% probability level. Some phenyl C atoms have been omitted for clarity.

dx.doi.org/10.1021/ic3004118 | *Inorg. Chem.* 2012, 51, 5427−5434

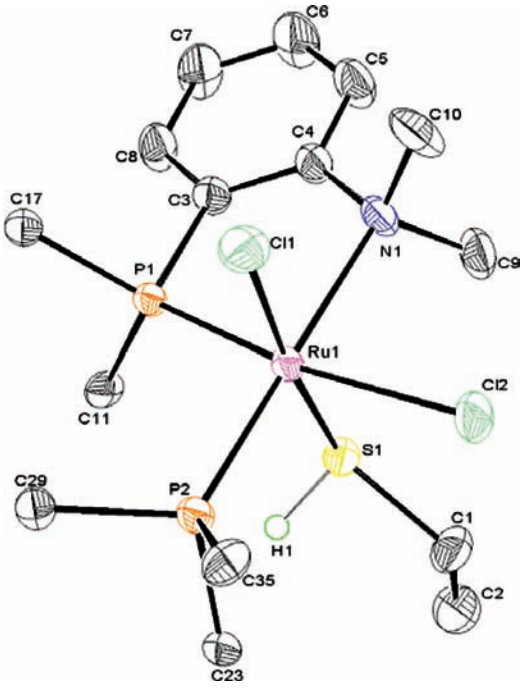

Figure 2. ORTEP plot for **4** with thermal ellipsoids shown at the 33% probability level. Some phenyl C atoms have been omitted for clarity.

Cl plane, and there is no hydrogen bonding between SH and the *cis*-Cl atom. The thiol H atom points toward the planes of the Ph groups: the H···C15 and H···C22 distances in **3** (2.84 and 2.49 Å, respectively), and the H···C11 and H···C24 distances in **4** (2.83 and 2.30 Å, respectively), indicate possible SH/π (phenyl rings) interactions,[5b,21] which may play a role in stabilizing the coordinated thiol.

The $^{31}P\{^{1}H\}$ NMR spectra of **3** and **4** in CD_2Cl_2 are consistent with the solid-state structures and are very similar to those of the H_2S adducts (see above). The spectra show an AX pattern for the *cis*-P atoms at δ ~51 and ~42 ($^{2}J_{PP}$ ~ 30 Hz), respectively, for the *P*–N and PPh_3 ligands. Of note, the binding of RSH and H_2S (eq 1) results in an initial vacant site trans to P_N becoming occupied by Cl, whereas the PR_3 ligand remains trans to the N atom, and this is reflected in an upfield shift of ~30 ppm for the P_N resonance, whereas that of the PR_3 ligand changes by <5 ppm. The ^{1}H NMR spectra of **3** (δ 3.35, 3.10) and **4** (δ 3.41, 3.24) reveal the expected inequivalence of the NMe groups. For **3**, the S(CH_3) and S*H* resonances overlap to give a multiplet at δ 0.70, but at −50 °C, these signals resolve into a doublet for S(CH_3) at δ 0.65 ($^{2}J_{HH}$ = 6.97) and a broad multiplet for S*H* at δ 0.60. For **4**, the coordinated S atom is chiral and the methylene CH_bH_c protons are diastereotopic, and hence anisochronous.[22] The ^{1}H NMR spectrum (Figure 3) shows multiplets at δ 2.00 and 0.88 for these protons, and the spectrum for the coordinated EtSH is nicely simulated using the *J* values given in Figure 4 for the various HH couplings and the $^{3}J_{HP}$ = 1.92 Hz coupling of the SH_a proton to the P_A atom. This *J* value is reasonable based on a Karplus relationship established within the P–Ru–S–H geometry of the isostructural *cis*-$RuCl_2(P{-}N)(PPh_3)(SH_2)$ species,[5b] noting in **4** the small dihedral angle of 69.81° between the P1–Ru–S and Ru–S–H1 planes. A $^{1}H\{^{31}P\}$NMR spectrum (Figure S1 in the Supporting Information) is thought to show that H_a is partially coupled to P1 (labeled P_A in Figure 3). The HH correlations were confirmed by a 2D COSY ^{1}H NMR experiment.

The solution, rt NMR spectra of **3**, **4**, and the isolated H_2S adducts (e.g., Figure 3) always show the presence of the precursor five-coordinate species (see eq 1), implying equilibrium reactions for these systems. The equilibrium constants for these reversible reactions and the associated thermodynamic data are considered later.

In Situ *cis*-$RuCl_2(P{-}N)(PPh_3)(R'SH)$ Species (R′ = ^{n}Pr, ^{i}Pr; ^{n}Pn, ^{n}Hx, Bn). Reactions of longer-chain thiols with $RuCl_2(P{-}N)(PPh_3)$ were also investigated, but attempts to isolate the products were unsuccessful because of the facile loss of R′SH and the O_2 sensitivity of the systems. However, the thiol species were readily detected in situ by $^{31}P\{^{1}H\}$ NMR spectra in $CDCl_3$ or C_6D_6; the addition of excess R′SH to the green solution of the precursor generated a yellow solution containing the product. The ^{1}H NMR spectra were uninformative because the product signals were obscured by those of excess thiol. The $^{31}P\{^{1}H\}$-AX patterns are like those of the H_2S, MeSH, and EtSH complexes and depend little on the nature of the thiol: all of the R′SH and H_2S species have $\delta(P_N)$ and $\delta(P)$ values in the respective ranges of 49–52 and 41–46 ppm, with $^{2}J_{PP}$ values of 29.5–30.5 Hz. The $^{31}P\{^{1}H\}$ NMR spectra of the R′ = ^{i}Pr and ^{n}Pn systems also revealed a further AX pattern in the same regions but with higher $^{2}J_{PP}$ values of 36.6 and 36.1 Hz, respectively; these spectra are tentatively assigned to the trans isomers, based on data for the *trans*-$RuCl_2(P{-}N)(PPh_3)(L)$ complexes, where L = H_2O, MeOH, and EtOH, which have $^{2}J_{PP}$ values of 36–38 Hz within the AX pattern.[6b] As seen qualitatively in the $^{31}P\{^{1}H\}$ NMR spectra, formation of the thiol species (eq 1) becomes less favorable with increasing bulk of the R′ group, and no reactions were observed with excess PhSH or thiophene.

IR and UV–vis Spectra. The vibration modes ν_3, ν_1, and ν_2 of gaseous H_2S (Scheme 1) are seen at 2629, 2615, and 1180 cm^{-1}, respectively.[23] For the Ru-SH_2 adducts **2a**,[5a] **2a**′,[5a] **2b**, and **2b**′ (see the Experimental Section), the ν_3 and ν_1 bands are observed at lower wavenumbers (in the 2506–2495 and 2476–2449 cm^{-1} regions), likely indicating a lengthening of the S–H bonds upon coordination, while ν_2 is obscured by other bands. For MeSH and EtSH, only the ν_1 stretch is observed (at 2580 and 2573 cm^{-1}, respectively),[24] and again this is lowered within the *cis*-$RuCl_2(P{-}N)(PPh_3)(R'SH)$ complexes **3** and **4** by ~47 cm^{-1} (R′ = Me) and ~57 cm^{-1} (R′ = Et). Limited data[5,6,7b,e]

Table 1. Selected Bond Lengths (Å) for 3 and 4 with Estimated Standard Deviations in Parentheses

	3	4		3	4
Ru1–S1	2.3393(8)	2.3397(5)	Ru1–Cl1	2.4238(8)	2.4210(5)
Ru1–P1	2.2802(8)	2.2743(4)	Ru1–Cl2	2.4470(8)	2.4678(5)
Ru1–P2	2.3109(8)	2.3110(5)	S1–H1	1.06(4)	1.28(2)
Ru1–N1	2.335(2)	2.3646(15)	S1–C39	1.802(3)	
			S1–C1		1.8243(19)
			C1–C2		1.510(3)

dx.doi.org/10.1021/ic3004118 | *Inorg. Chem.* 2012, 51, 5427–5434

Table 2. Selected Bond Angles (deg) for 3 and 4 with Estimated Standard Deviations in Parentheses

	3	4		3	4
H1−S1−C39	99(2)		S1−Ru1−P1	86.14(3)	87.383(17)
H1−S1−C1		94.4(11)	S1−Ru1−P2	94.85(3)	97.191(16)
Ru1−S1−H1	102(2)	109.1(11)	S1−Ru1−N1	87.08(7)	85.34(4)
Ru1−S1−C39	116.50(12)		Cl2−Ru1−P1	169.27(3)	167.859(17)
Ru1−S1−C1		115.85(8)	Cl2−Ru1−P2	86.70(3)	91.766(16)
Cl1−Ru1−S1	176.60(3)	174.610(16)	Cl2−Ru1−N1	86.52(6)	86.30(4)
Cl1−Ru1−P1	92.51(3)	96.246(17)	P1−Ru1−N1	83.26(6)	82.48(4)
Cl1−Ru1−P2	88.50(3)	86.154(17)	P2−Ru1−N1	172.96(7)	176.74(4)
Cl1−Ru1−N1	89.67(7)	91.17(4)	S1−C1−C2		109.49(17)
Cl1−Ru1−Cl2	90.68(3)	88.584(17)			

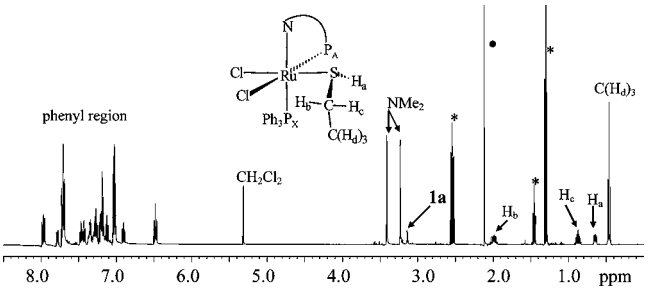

Figure 3. ^{1}H NMR spectrum (500 MHz) of **4** in CD_2Cl_2 at 20 °C. Note: **4** is in equilibrium with **1a** (δ 3.13, s, NMe_2) and free EtSH (*) (δ 2.55 dq, $HSCH_2CH_3$; δ 1.46, t, $HSCH_2$; δ 1.31, t, (CH_2CH_3)); acetone (●) (δ 2.1, s).

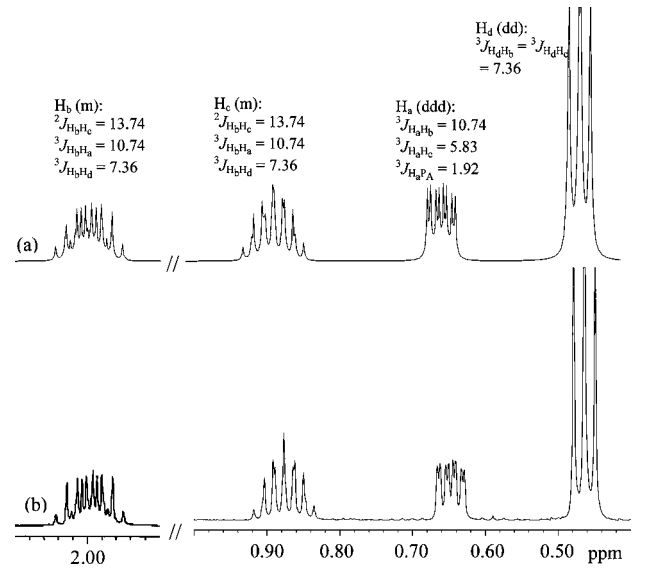

Figure 4. ^{1}H NMR spectra of coordinated EtSH of complex **4** (500 MHz, CD_2Cl_2): (a) simulated spectrum, J values in Hz; (b) expanded regions of the actual spectrum (Figure 3).

Scheme 1

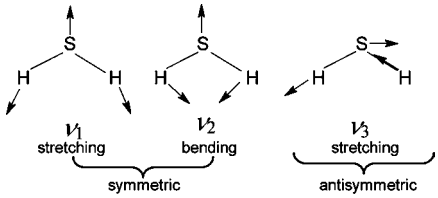

suggest that coordination of R′SH or H_2S to Ru^{II} always results in a lowering of the ν_{SH} values. In $Ru(SH_2)(PPh_3)$("S_4")·THF, where "S_4" is the dianion 1,2-bis[(2-mercaptophenyl)thio]-ethane, the decrease in the ν values by 200−350 cm^{-1} seems exceptional and is likely due to the presence of S−H···S and S−H···O hydrogen bridges.[25] Surprisingly, the ν_1 and ν_3 values for **2a** and **2b** are the same (2506 and 2476 cm^{-1}, respectively), as are the values for **2a**′ and **2b**′ (2495 and 2449 cm^{-1}), showing that the substitution of Cl^- by Br^- has no effect on the S−H stretching modes, whereas the replacement of PPh_3 by $P(p\text{-tolyl})_3$ within the chloro species decreases these bands by ∼10 and ∼25 cm^{-1}, respectively,[5,6] possibly because of increased SH/π interactions within the ring system of the p-tolyl group. Unfortunately, a direct comparison between the two structures[5] cannot be made because only one H atom of the H_2S ligand was located in the $P(p\text{-tolyl})_3$ complex.[5a]

The green $RuX_2(P{-}N)(PR_3)$ complexes in CH_2Cl_2 have visible absorption bands in the ranges 452−512 nm (λ_1; ε_1 ∼ 780−1170 M^{-1} cm^{-1}) and 672−780 nm (λ_2; ε_2 ∼ 435−615 M^{-1} cm^{-1}; Table S and Figure S2 in the Supporting Information). The binding of R′SH (R′ = H, Me, Et) gives yellow products that show a blue shift of λ_1 by up to ∼30 nm (with ε_1 values decreased by ∼25%), while λ_2 is no longer seen in the 530−820 nm region. The ε values and observed trend for both λ_1 and λ_2, where the band energies decrease in the sequence Cl > Br > I (Table S in the Supporting Information), indicate that the bands likely result from Ru^{II}-to-P-ligand charge-transfer transitions aided by π donation from the halide ligands. Coordination of the S ligands perhaps shifts the λ_2 band to lower energy. Attempts to investigate kinetics via the UV−vis spectral changes were unsuccessful because of the "instantaneous" reactions even at −10 °C; data obtained by stopped-flow experiments, even with attempted rigorous exclusion of air, were irreproducible because of decomposition of the reactant and/or products. Equilibrium constants were, however, readily measured under Ar via NMR data acquired in J. Young NMR tubes.

Thermodynamics for Reversible Formation of the H_2S and Thiol Complexes. The equilibrium constants (K) were determined for the reversible binding of H_2S and R′SH (eq 2; R′ = H, Me, Et) using ^{1}H NMR integration data for each species in C_6D_6; better resolved peaks were seen in this solvent

$$\textit{trans}\text{-}RuCl_2(P{-}N)(PPh_3)\ (\mathbf{1a}) + R'SH \overset{K}{\rightleftarrows} \textit{cis}\text{-}RuCl_2(P{-}N)(PPh_3)(R'SH) \quad (2)$$

(vs CD_2Cl_2 or $CDCl_3$) over the temperature range used (13−75 °C). The determination of K is illustrated by a consideration of Figure 5, which shows data for dissociation of *cis*-$RuCl_2$(P−

dx.doi.org/10.1021/ic3004118 | Inorg. Chem. 2012, 51, 5427−5434

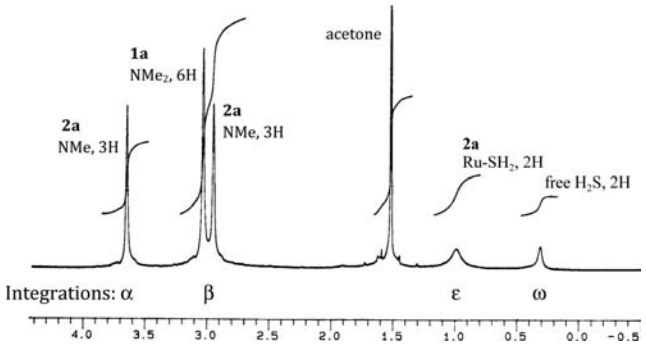

Figure 5. ^{1}H NMR spectra in the region δ −0.5 to +4.5 (300 MHz, C_6D_6) for the equilibrium established (by dissolution of the acetone solvate of **2a**) between **2a**, **1a**, and H_2S at ∼20 °C. The acetone signal in C_6D_6 is ∼0.5 ppm upfield from that in $CDCl_3$ and CD_2Cl_2 (see ^{1}H NMR data for the isolated acetone solvates of **2b′**, **3**, and **4**).

N)(PPh$_3$)(SH$_2$) (**2a**) to form some **1a**, where K = [**2a**]/[**1a**][H_2S]. The samples for analysis were prepared by dissolving the acetone solvate of **2a** in C_6D_6 under Ar. As the temperature is raised, the integrations of the ^{1}H signals of **1a** (δ 3.07, NMe_2) and free H_2S (δ 0.30) increase, while those of **2a** (δ 3.67, 2.97, NMe_2) and RuSH_2 (δ 1.02) decrease; this shows qualitatively that the formation of **2a** is exothermic. Because $[Ru]_{total}$ is known (= [**1a**] + [**2a**]) and defining x as [**2a**]/[**1a**] and y = **1a**/$[H_2S]_{solution}$, K can be written as $xy(1 + x)/[Ru]_{total}$; labeling the integrated peak areas in Figure 5 as α, β, ε, and ω gives rise to the expressions shown in eq 3 from which x and y (and, hence, K) can be calculated. Raw data for the equilibrium

$$x = \frac{\alpha/3 \text{ (or } \varepsilon/2)}{(\beta - \alpha)/6}; \quad y = \frac{(\beta - \alpha)/6}{\omega/2} \tag{3}$$

calculations involving three isolated H_2S species and the isolated MeSH and EtSH complexes (where similar calculations apply) are given in the Appendix in the Supporting Information. The K values and corresponding $\Delta H°$, $\Delta S°$, and $\Delta G°$ values determined by van't Hoff plots (Figure S3 in the Supporting Information) are summarized in Table 3. We are unaware of any other thermodynamic data reported upon coordination of H_2S or thiols to transition metals.

The negative $\Delta S°$ values are consistent with the binding of a small molecule to a metal site, while the low-value exothermicities imply relatively weak Ru−S bond energies; this excludes consideration of energy changes in the trans-to-cis halide rearrangement that accompanies the forward reaction (see below). The relative K values at 25 °C show that the MeSH complex **3** is the most stable, and qualitative visual observations and UV−vis data confirm this: upon dissolution of this complex, the color remains yellow, characteristic of **3**, whereas dissolution of the H_2S and EtSH complexes gives a green color due to the presence of **1a**. The K values of the H_2S adducts **2a** and **2b** are also consistent with the usually observed greater trans influence of Br^- versus Cl^-.[26] Of note, within all of the systems, increasing exothermicity is accompanied by increasingly unfavorable entropic changes, yet a further example of the commonly observed "compensation effect";[27] indeed, the data of Table 3 give a good linear plot of $-\Delta H°$ versus $-\Delta S°$ (Figure S4 in the Supporting Information).

Enthalpy changes for the reverse reaction of eq 2 in the solid state were obtained by DSC. Solid samples of the acetone-solvated **2a**, **3**, and **4** complexes were heated in the DSC chamber under N_2, and the endothermic $\Delta H°$ values were measured for the loss of H_2S, MeSH, and EtSH, ignoring the loss of acetone (Figure 6). The Ru−S bond strength in **4** is the weakest, possibly because of the larger EtSH ligand. Consistent with this, the exothermicity for the formation of **4** in solution is also the lowest value (Table 3), but the respective $\Delta H°$ values determined in solution are up to 60% lower than those in the solid state, and this is tentatively attributed to the enthalpy change of a cis-to-trans dichloro isomerization process in solution. When the yellow, solid samples of **2a**, **3**, and **4** are heated under vacuum at 50 °C for over 2 h, the S ligands are removed to give a green product, which upon exposure to air rapidly decomposes to an uncharacterizable black powder. This green product is different from the more aerobically stable **1a** and is thought to be mainly the cis isomer, as judged by far-IR data: the trans isomer has its major band at 336 cm^{-1} (presumably ν_{RuCl}), whereas the presumed cis isomer shows several bands in the 329−303 cm^{-1} region and no band at 336 cm^{-1}. Dissolution of this cis isomer in $CDCl_3$ results in the rapid formation of the trans isomer **1a**, as observed by NMR spectroscopy. A comparison of the solution and solid-state enthalpy values (ignoring any solvation effects in the solution equilibria) gives, for conversion of the cis isomer to the more thermodynamically stable trans isomer **1a**, $\Delta H°$ values of −39 to −66 kJ mol^{-1} within the five-coordinate species. These

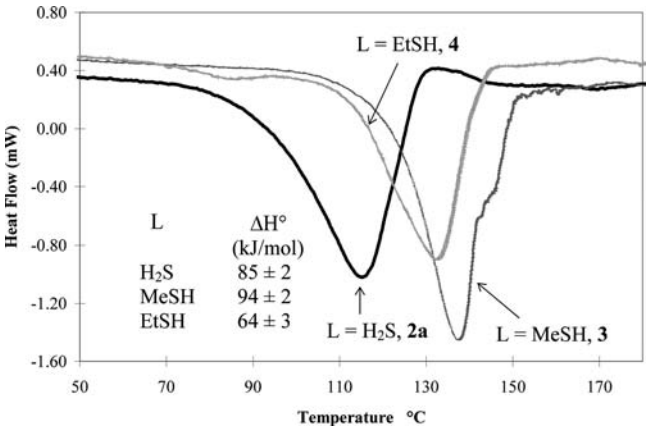

Figure 6. DSC curves for *cis*-RuCl_2(P−N)(PPh_3)(L) complexes. Samples are heated in an N_2 atmosphere (flow rate = 40 cm^3 min^{-1}) at a rate of 5 °C min^{-1} to 200 °C.

Table 3. Thermodynamic Data at 25 °C for the Formation of *cis*-RuX_2(P−N)(PR_3)(L) Complexes in C_6D_6 (eq 2)

RuX_2(P−N)(PR_3)(L)	K (M^{-1})[a]	$\Delta G°$ (kJ mol^{-1})	$\Delta H°$[b] (kJ mol^{-1})	$\Delta S°$[b] (J mol^{-1} K^{-1})
X = Cl, R = Ph, L = H_2S (**2a**)	153 ± 5	−12.5 ± 0.1	−46 ± 4	−112 ± 14
X = Br, R = Ph, L = H_2S (**2b**)	51 ± 4	−9.7 ± 0.2	−33 ± 4	−77 ± 13
X = Cl, R = *p*-tolyl, L = H_2S (**2a′**)	120 ± 15	−11.9 ± 0.3	−54 ± 9	−140 ± 35
X = Cl, R = Ph, L = MeSH (**3**)	296 ± 20	−14.1 ± 0.2	−28 ± 3	−48 ± 10
X = Cl, R = Ph, L = EtSH (**4**)	154 ± 8	−12.5 ± 0.1	−22 ± 4	−32 ± 14

[a]Error values estimated from repeat experiments. [b]Errors for $\Delta H°$ and $\Delta S°$ estimated from maximum and minimum slopes and intercepts of van't Hoff plots, respectively.

dx.doi.org/10.1021/ic3004118 | *Inorg. Chem.* 2012, 51, 5427−5434

values are of the same order of magnitude as those reported for the solid-phase isomerizations of the chloride ligands within the six-coordinate $RuCl_2(CO)(PR)_3$ complexes ($\Delta H°$ = 15, 21, and 48 kJ mol^{-1} for the R = Ph_2Me, $PhMe_2$, and Me_3 species, respectively).[28]

Compound 5. When green CH_2Cl_2 or C_6H_6 solutions of **1a** are exposed to O_2, the color intensifies, and after ∼1 h of reaction time, the addition of hexanes precipitates the dark-blue-green complex **5**, μ-dichloro-μ-oxobis[chloro(*o*-diphenylphosphino-*N*,*N*′-dimethylaniline)ruthenium(III), which was isolated in ∼30% yield; crystals of an acetone solvate were obtained from acetone solutions. The X-ray structure of **5** was briefly reported in a communication from our group that described the formation of **5** via decomposition of *cis*-$RuCl_2(P{-}N)(PPh_3)(N_2O)$.[4b]

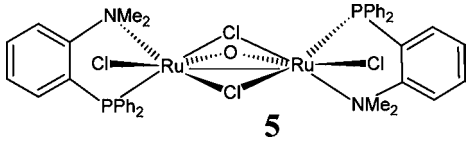

5

The ORTEP plot and key geometric parameters have been published,[4b] but no discussion of the structure was presented. Each Ru has pseudooctahedral geometry, being coordinated to one P−N ligand, one terminal Cl, two μ-Cl ligands, and one μ-O ligand. The Ru−Ru distance (2.92 Å) is typical of a Ru−Ru single bond (2.632−3.034 Å),[29] implying the presence of a $Ru^{III}{-}O{-}Ru^{III}$ moiety. The metal−metal bond results in reduced bond angles at the μ-Cl (71.25 and 71.92°) and μ-O (98.6°) ligands; in complexes with longer Ru−Ru distances, such angles are significantly larger (e.g., a $Ru^{III}{-}O{-}Ru^{III}$ angle of 122.3° is seen in a complex with a Ru−Ru distance of 3.266 Å).[30] The Ru−O bond lengths (both 1.92 Å) are up to ∼0.1 Å longer than those of other reported $(\mu\text{-}O)Ru^{III}{}_2$ species (1.80−1.90 Å)[30,31] and are ∼0.1 Å shorter than those in $Ru^{III}{}_2$-μ-OH and $Ru^{III}{}_2$-μ-OH_2 complexes.[32,33] The O atom is centered equally between the Ru atoms, but the Ru−μ-Cl lengths reveal the trans influence of the P atom in that the Ru1−Cl1 and Ru2−Cl2 distances, where the Cl atoms are trans to the P atoms, are ∼0.2 Å longer than the Ru1−Cl2 and Ru2−Cl1 bonds, where the Cl atoms are trans to the N atoms. This same effect has also been seen in $Ru^{II}{}_2(\mu\text{-}Cl)_2$ species.[34] Complex **5** is diamagnetic, as evidenced by a magnetic susceptibility measurement; the spin coupling may result from a Ru−Ru interaction, but strong electronic coupling between the low-spin d^5 Ru^{III} ions through the oxo bridge and the relatively small Ru−O−Ru angle cannot be ruled out.[31a,35]

Solution NMR data in C_6D_6 for **5** show an AB pattern for the P atoms with coupling through four bonds ($^4J_{PP}$ = 10.4 Hz) and four singlets for inequivalent NMe groups. The UV−vis spectrum in dimethyl sulfoxide shows intense LMCT bands at 348 (ε = 15300 M^{-1} cm^{-1}) and 652 nm (ε = 11200 M^{-1} cm^{-1}); the data resemble those for other $Ru^{III}{}_2$ species with bridging ligands.[31a,b,35]

O_2 (and not trace water) is needed for the formation of **5**. An in situ reaction of **1a** and O_2 in C_6D_6 at rt to form **5** also generates O=PPh_3 (δ_P 25.41), and indeed **1a** will catalyze the O_2 oxidation of added PPh_3 to the oxide before any **5** is detected.

The H_2S complexes are also very O_2-sensitive in solution. When O_2 is added to a yellow $CDCl_3$ solution of **2a** under 1 atm of H_2S at rt, a dark-green solution is again formed rapidly, but the addition of hexanes now results in a green-brown solid (different from **5**) that gives broad $^{31}P\{^1H\}$ and ^1H NMR signals. Evaporation of the solvents from the filtrate allowed for isolation of a white solid, shown to be S=PPh_3, which was characterized by elemental analysis and $^{31}P\{^1H\}$ data in $CDCl_3$ (δ 44.8). Of interest, when a mixture of O_2 and H_2S (∼1:1 by volume injection) is added to a CH_2Cl_2 solution of **2a** and a 25-fold excess of PPh_3, the ruthenium complex before decomposition catalytically converts in ∼20 min all of PPh_3 to S=PPh_3, with water as the coproduct. The reaction, shown in eq 4, likely offers a new but impractical method for the synthesis of phosphine sulfides!

$$H_2S + PPh_3 + \frac{1}{2}O_2 \xrightarrow{Ru} SPPh_3 + H_2O \quad (4)$$

CONCLUSIONS

The reversible binding of thiols to a five-coordinate ruthenium(II) complex is described, as well as further examples of H_2S complexes of a type previously reported by our group. Crystal structures of the MeSH and EtSH complexes are presented; the former is the first example of a structurally characterized transition metal−MeSH complex, which (to the best of our knowledge) has the shortest S−H bond length yet reported for any metal−thiol complex. The NMR, IR, and UV−vis spectra of the adducts are consistent with their formulations, and thermodynamic data of their formation reveal $\Delta H°$ values in the range of −30 to −55 kJ mol^{-1} for H_2S bonding and −20 to −30 kJ mol^{-1} for the thiols, implying relatively weak Ru−S bond energies; the $\Delta S°$ values are negative, as expected. Whereas *trans*-$RuCl_2(P{-}N)(PPh_3)$ decomposes in air to the known complex **5** and $OPPh_3$, *cis*-$RuCl_2(P{-}N)(PPh_3)(SH_2)$ can catalyze the O_2 oxidation of a mixture of H_2S and PPh_3 to H_2O and $SPPh_3$.

ASSOCIATED CONTENT

Supporting Information

X-ray crystallographic data for the structures of **3** and **4** (CIF files), UV−vis data for the MeSH, EtSH, and H_2S adducts, ^1H NMR signal for the S−H_a proton in **4**, detailed data for the *K* equilibria and van't Hoff plots, and the compensation effect plot. This material is available free of charge via the Internet at http://pubs.acs.org.

AUTHOR INFORMATION

Corresponding Author

*E-mail: brj@chem.ubc.ca.

Notes

The authors declare no competing financial interest.

†Deceased October 27, 1998.

ACKNOWLEDGMENTS

We thank the Natural Sciences and Engineering Council of Canada for financial support and Colonial Metals Inc. for a loan of $RuCl_3{\cdot}xH_2O$.

REFERENCES

(1) Rebouças, J. S.; Patrick, B. O.; James, B. R. *J. Am. Chem. Soc.* **2012**, *134*, 3555.

(2) See refs 1−3, 10, 11, and 17−20 given in the above paper.

(3) For example: (a) James, B. R. *Pure Appl. Chem.* **1997**, *69*, 2213 and references cited therein. (b) Coto, A.; de los Ríos, I.; Tenorio, M. J.; Puerta, M. C.; Valerga, P. *J. Chem. Soc., Dalton Trans.* **1999**, 4309. (c) Schwarz, D. E.; Dopke, J. A.; Rauchfuss, T. B.; Wilson, S. R. *Angew.*

Chem., Int. Ed. **2001**, *40*, 2351. (d) McGuire, D. G.; Khan, M. A.; Ashby, M. T. *Inorg. Chem.* **2002**, *41*, 2202. (e) Pamplin, C. B.; Rettig, S. J.; Patrick, B. O.; James, B. R. *Inorg. Chem.* **2011**, *50*, 8094 and references cited therein.

(4) (a) Mudalige, D. C.; Rettig, S. J.; James, B. R.; Cullen, W. R. *J. Chem. Soc., Chem. Commun.* **1993**, 830. (b) Pamplin, C. B.; Ma, E. S. F.; Safari, N.; Rettig, S. J.; James, B. R. *J. Am. Chem. Soc.* **2001**, *123*, 8596.

(5) (a) Mudalige, D. C.; Ma, E. S.; Rettig, S. J.; James, B. R.; Cullen, W. R. *Inorg. Chem.* **1997**, *36*, 5426. (b) Ma, E. S.; Rettig, S. J.; James, B. R. *Chem. Commun.* **1999**, 2463.

(6) (a) Mudalige, D. C. Ph.D. Dissertation, The University of British Columbia, Vancouver, British Columbia, Canada, 1994. (b) Ma, E. S. Ph.D. Dissertation, The University of British Columbia, Vancouver, British Columbia, Canada, 1999. (c) Ma, E. S.; Mudalige, D. C.; James, B. R. 7th International Conference on the Chemistry of Pt Group Metals, Nottingham, U.K., 1999; Abstract I.25.

(7) (a) Amarasekera, J.; Rauchfuss, T. B. *Inorg. Chem.* **1989**, *28*, 3875. (b) Conroy- Lewis, F. M.; Simpson, S. J. *J. Chem. Soc., Chem. Commun.* **1991**, 388. (c) Treichel, P. M.; Crane, R. A.; Haller, K. N. *J. Organomet. Chem.* **1991**, *401*, 173. (d) Treichel, P. M.; Schmidt, M. S.; Crane, R. A. *Inorg. Chem.* **1991**, *30*, 379. (e) Park, H.; Minick, D.; Draganjac, M.; Cordes, A. W.; Hallford, R. L.; Eggleton, G. *Inorg. Chim. Acta* **1993**, *204*, 195. (f) Park, H.; Minick, D.; Draganjac, M.; Crump, J. W.; Cordes, A. W.; Holt, E. M. *Proc. Arkansas Acad. Sci.* **1993**, *47*, 142. (g) Jiang, Y.; Draganjac, M.; Cordes, A. W. *J. Chem. Crystallogr.* **1995**, *25*, 653. (h) Shaw, A. P.; Ryland, B. L.; Norton, J. R.; Buccella, D.; Moscatelli, A. *Inorg. Chem.* **2007**, *46*, 5805.

(8) (a) Jazzar, R. F. R.; Bhatia, P. H.; Mahon, M. F.; Whittlesey, M. K. *Organometallics* **2003**, *22*, 670. (b) Chatwin, S. L.; Davidson, M. G.; Doherty, C.; Donald, S. M.; Jazzar, R. F. R.; Macgregor, S. A.; McIntyre, G. J.; Mahon, M. F.; Whittlesey, M. K. *Organometallics* **2006**, *25*, 99.

(9) Li, Y.; Huang, J.-S.; Xu, G.-B.; Zhu, N.; Zhou, Z.-Y.; Che, C.-M.; Wong, K.-Y. *Chem.—Eur. J.* **2004**, *10*, 3486.

(10) Belchem, G.; Steed, J. W.; Tocher, D. A. *J. Chem. Soc., Dalton Trans.* **1994**, 1949.

(11) Bartucz, T. Y.; Golombek, A.; Lough, A. J.; Maltby, P. A.; Morris, R. H.; Ramachandran, R.; Schlaf, M. *Inorg. Chem.* **1998**, *37*, 1555.

(12) Schlaf, M.; Lough, A. J.; Morris, R. H. *Organometallics* **1996**, *15*, 4423.

(13) Perrin, D. D.; Armarego, W. L. F.; Perrin, D. R. *Purification of Laboratory Chemicals*, 2nd ed.; Pergamon: Oxford, U.K., 1980.

(14) Hallman, P. S.; Stephenson, T. A.; Wilkinson, G. *Inorg. Synth.* **1970**, *12*, 237.

(15) Armit, P. W.; Sime, W. J.; Stephenson, T. A.; Scott, L. *J. Organomet. Chem.* **1978**, *161*, 391.

(16) *d*TREK. Area Detector Software*, version 4.13; Molecular Structure Corp.: The Woodlands, TX, 1996−1998.

(17) Altomare, A.; Burla, M. C.; Camalli, M.; Cascarano, G. L.; Giacovazzo, C.; Guagliardi, A.; Moliterni, A. G. G.; Polidori, G.; Spagna, R. *J. Appl. Crystallogr.* **1999**, *32*, 115.

(18) Sheldrick, G. M. *Acta Crystallogr.* **2008**, *A64*, 112.

(19) *WinGX* V1.80.05: Farrugia, L. J. *J. Appl. Crystallogr.* **1999**, *32*, 837.

(20) (a) Peruzzini, M.; de los Ríos, I.; Romerosa, A. *Prog. Inorg. Chem.* **2001**, *49*, 169. (b) Chatwin, S. L.; Diggle, R. A.; Jazzar, R. F. R.; MacGregor, S. A.; Mahon, M. F.; Whittlesey, M. K. *Inorg. Chem.* **2003**, *42*, 7695.

(21) Osakada, K.; Yamamoto, T.; Yamamoto, A. *Inorg. Chim. Acta* **1985**, *105*, L9.

(22) James, B. R.; Pacheco, A.; Rettig, S. J.; Ibers, J. A. *Inorg. Chem.* **1988**, *27*, 2414 and references cited therein.

(23) (a) Allen, H. C.; Blaine, L. R.; Plyler, E. K.; Cross, P. C. *J. Chem. Phys.* **1956**, *24*, 35. (b) Allen, H. C.; Plyler, E. K. *J. Chem. Phys.* **1956**, *25*, 1132.

(24) Csizmadia, I. G. In *The Chemistry of the Thiol Group*; Patai, S., Ed.; John Wiley & Sons: Toronto, Canada, 1974; Part I, p 7.

(25) (a) Sellmann, D.; Lechner, P.; Knoch, F.; Moll, M. *Angew. Chem., Int. Ed. Engl.* **1991**, *30*, 552. (b) Sellmann, D.; Lechner, P.; Knoch, F.; Moll, M. *J. Am. Chem. Soc.* **1992**, *114*, 922.

(26) Appleton, T.; Clark, H. C.; Manzer, L. *Coord. Chem. Rev.* **1973**, *10*, 335.

(27) For example: (a) Fishman, A. I.; Stolov, A. A.; Remizov, A. B. *Spectrochim. Acta A* **1990**, *46*, 1037. (b) Liu, Y.; Han, B.-H.; Li, B.; Zhang, Y.-M.; Zhao, P.; Chen, Y.-T.; Wada, T.; Inoue, Y. *J. Org. Chem.* **1998**, *63*, 1444. (c) Cornish-Bowden, A. *J. Biosci.* **2002**, *27*, 121. (d) Ruvolo-Filho, A.; Curti, P. S. *Ind. Eng. Chem. Res.* **2006**, *45*, 7985. (e) Treuheit, N. A.; Beach, M. A.; Komives, E. A. *Biochemistry* **2011**, *50*, 4590.

(28) Krassowski, D. W.; Reimer, K.; LeMay, H. E., Jr.; Nelson, J. H. *Inorg. Chem.* **1988**, *27*, 4307.

(29) Knox, S. A. R.; Macpherson, K. A.; Orpen, A. G.; Rendle, M. C. *J. Chem. Soc., Dalton Trans.* **1989**, 1807.

(30) Sudha, C.; Mandal, S. K.; Chakravarty, A. R. *Inorg. Chem.* **1993**, *32*, 3801.

(31) For example: (a) Llobet, A.; Curry, M. E.; Evans, H. T.; Meyer, T. J. *Inorg. Chem.* **1989**, *28*, 3131. (b) Saski, Y.; Suzuki, M.; Nagasawa, A.; Tokiwa, A.; Ebihara, M.; Yamaguchi, T.; Kabuto, C.; Ochi, T.; Ito, T. *Inorg. Chem.* **1991**, *30*, 4903. (c) Ishitani, O.; White, P. S.; Meyer, T. J. *Inorg. Chem.* **1996**, *35*, 2167. (d) Wang, W.-Z.; Liu, X.; Liao, D.-Z.; Jiang, Z.-H.; Yan, S.-P.; Wang, G.-L. *Inorg. Chem. Commun.* **2002**, *5*, 1007. (e) Ye, H.-Y.; Chen, J.-L.; Chen, Z.-N. *Inorg. Chem. Commun.* **2007**, *10*, 1023.

(32) Orpen, A. G.; Brammer, L.; Allen, F. H.; Kennard, O.; Watson, D. G.; Raylor, R. *J. Chem. Soc., Dalton Trans.* **1989**, S1.

(33) Zhilyaev, A. N.; Kuz'menko, I. V.; Fomina, T. A.; Katser, S. B.; Baranovskii, I. B. *Russ. J. Inorg. Chem. (Engl. Transl.)* **1993**, *38*, 847.

(34) MacFarlane, K. S.; Thorburn, I. S.; Cyr, P. W.; Chau, D. E. K.-Y.; Rettig, S. J.; James, B. R. *Inorg. Chim. Acta* **1998**, *270*, 130.

(35) Weaver, T. R.; Meyer, T. J.; Adeyemi, S. A.; Brown, G. M.; Eckberg, R. P.; Hatfield, W. E.; Johnson, E. C.; Murray, R. W.; Untereker, D. *J. Am. Chem. Soc.* **1975**, *97*, 3039.